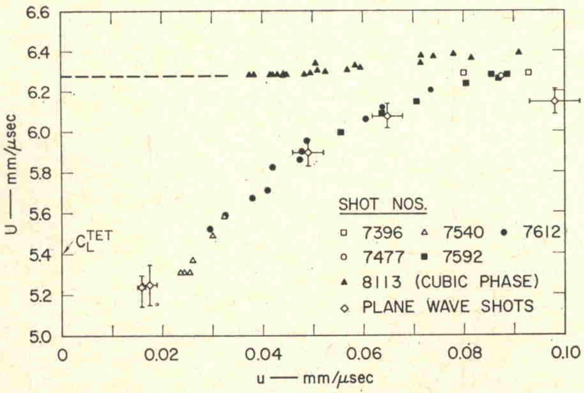

FIG. 5. Shock velocity vs particle velocity for $BaTiO_3$ (5% $CaTiO_3$) at low pressure ($u=\frac{1}{2}\mu_{fs} \div \cos\gamma$, where γ=angle of incidence).

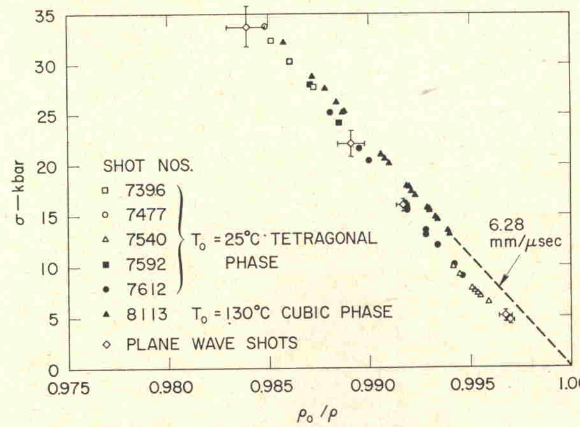

FIG. 7. Shock pressure vs compression for $BaTiO_3$ (5% $CaTiO_3$) at low pressure.

creased in discrete steps. These steps are interpreted as "reverberations" of the first (~30 kbar) wave between the oncoming second wave and the free surface. That is, the mechanism giving rise to the original two-wave system is assumed to remain active in material which has been compressed and subsequently rarefied by the first wave and its reflection from the free surface, respectively. On this model, the second shock velocity U_2 is calculated from Eq. (1), whose derivation is clear from Fig. 8:

$$U_2=x_2/t=U_1[3U_1t_1-(U_1-u_1)t_2']/[(U_1+u_1)t_1+U_1t_2']. \qquad (1)$$

The resulting values of U_2 have been used to compute the 149- and 167-kbar points. A similar treatment does not affect the 310-kbar point.

Most of the intermediate pressure points were deduced from the shot employing oblique geometry (see Table II). The precision of these data is not high because of uncertainties in the analysis, e.g., the values of U_2 represent an average of the loci of the points labeled 5 and 6 in Table II; any influence of the reflected first wave is ignored. It is worth emphasizing, however, that the optical lever technique worked well on this bare, polished ceramic well above its elastic limit and that multiple wavefronts were clearly resolved.

As the shock strength drops below 30 kbar, the shock velocity decreases to ~5.3 mm/μsec at 7 kbar. This was the lowest attainable pressure in oblique geometry, corresponding to the minimum possible ratio of explosive thickness to specimen thickness. Two plane-wave shots at ~5 kbar, utilizing optical lever recording, gave 5.2 mm/μsec. In one of these, in which the elastic wave in annealed Armco iron (measured amplitude of 8 kbar) was used to drive the specimen, a low-amplitude (<1 kbar) "foot" propagating at approximately c_L was observed to precede the wave produced in the BT.

The oblique shot fired at elevated temperature provided data in the range from 13 to 30 kbar for the paraelectric phase of BT; the corresponding wave velocity range was 6.28–6.38 mm/μsec, nearly constant, in contrast to the room temperature results. An accu-

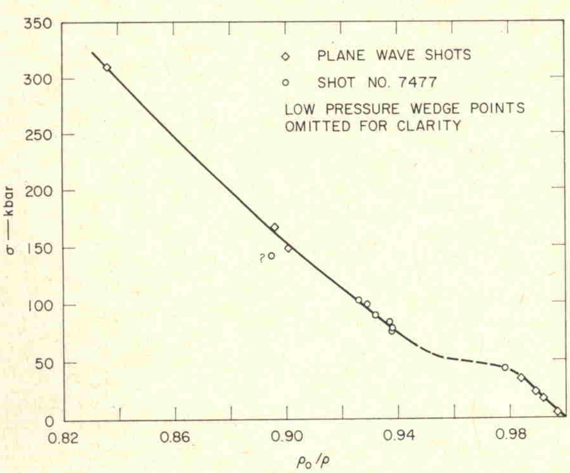

FIG. 6. Shock pressure vs compression for $BaTiO_3$ (5% $CaTiO_3$).

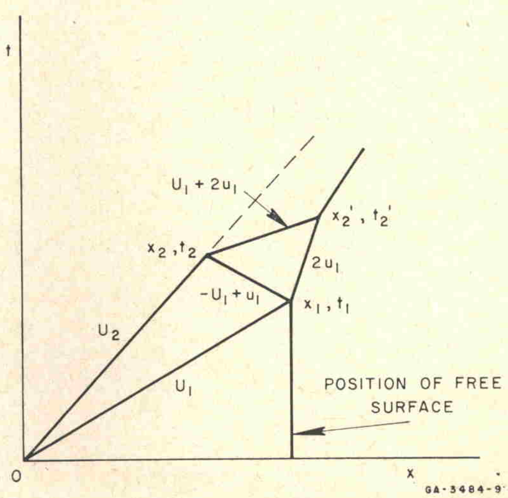

FIG. 8. Illustration of alternative calculation of U_2.

TABLE III. Summary of data for 95/5 PZT.

DRIVER			SPECIMEN			TYPE OF FREE-SURFACE MEASUREMENT[a]	FIRST WAVE					SECOND WAVE[b]					
erial	Thickness (mm)	Press. (kbar)	Desig- nation	Density (g/cm^3)	Nominal Thickness (mm)		U_1 (mm/μsec)	u_1 (mm/μsec)	σ_1 (kbar)	ρ_0/ρ	v_1 (cm^3/g)	U_2 (mm/μsec)	u_2 (mm/μsec)	σ_2 (kbar)	ρ_0/ρ	v_2 (cm^3/g)	
Al	12.5	133[d]	9 7a	7.88 7.87	12.1 7.6 max (6° wedge)	I.M. O.L.	-- --	-- --	-- --	-- --	-- --	4.52 4.53	(0.4)[e] --	142 --	0.912 --	0.1158 --	u_{fs} increases a Traces diffuse
Al	12.5	125[d]	7b	7.87	7.4 max (6½° wedge)	O.L.	--	--	--	--	--	4.60	--	--	--	--	Traces diffuse.
+ te + + te +	Each 6	26	6	7.74	12.3	I.M.	(3.55)	0.095	(26)	(0.9732)	(0.1257)	--	--	--	--	--	Evidence of 4.1 due to elastic
+ te +	Each 6	65	2	7.81	12.5	I.M.	4.14	0.123	41	0.970	0.1242	(3.5)	0.235	(70)	(0.938)	(0.1201)	
led Fe	26[g] (6° taper)	7.9	8	7.82	6.7	I.M.	4.26[h]	0.127	42	0.970	0.1241	--	--	--	--	--	
Al	12.5	136	5	7.68	12.5	I.M.	--	--	--	--	--	4.15	0.448	142	0.8925	0.1161	u_{fs} increases a
steel ite	12.5 ~12.5 (2° taper)	27[d]	11	7.77	6.6	I.M.	4.12	(0.150)	(48)	(0.9636)	(0.1240)	--	--	--	--	--	Poor record.
	12.5	150[d]	1	7.73	5.3	I.M.	--	--	--	--	--	4.24	0.435	142	0.8973	0.1161	
Al ite	12.5 ~11.4 (2° taper)	117 in brass	13	7.89	5.1	I.M.	4.36	0.125	43	0.9713	0.1232	4.04	0.323	106	0.9222	0.1169	
Al ite	12.5 ~11.4 (2° taper)	125 in brass Spec.	13	7.89	6.5 max (9° wedge)	O.L.	4.26	0.145	48	0.9657	0.1221	4.00	0.355	115	0.9130	0.1159	
steel	41 mm[g] (10° taper)	18	17	7.80	5.4	O.L.	4.22 3.55	0.0073 0.042	2.4 12.1	0.9983 0.989	0.1280 0.1268	-- --	-- --	-- --	-- --	-- --	u_{fs} approx. dou arrivals.
+ e	12.5 ~12.5 (2° taper)	32[d]	12	7.67	5.6 max (12° wedge)	O.L.	4.03	(0.12 to 0.065)	(38 to 21)	(0.970 to 0.983)	(0.1265 to 0.1282)	--	--	--	--	--	Poor record.
			24	7.81	6.6	O.L.	4.19	(0.115)	(38)	(0.972)	(0.1244)	--	--	--	--	--	Poor record.
+ e	12.5 ~12.5 (2° taper)	32[d]	23	7.74	6.6 max (7° wedge)	O.L.	4.12	(0.125)	(39)	(0.970)	(0.1253)	--	--	--	--	--	Poor record.
steel	38[g] (10° taper)	19	17	7.80	3.6	O.L.	4.26 3.62	0.0062 0.072	2.04 21.1	0.9986 0.9811	0.1280 0.1258	-- --	-- --	-- --	-- --	-- --	u_{fs} triples betw
	43[g]	21	23	7.74	4.5	O.L.	4.15 3.59	0.0046 0.0725	1.5 20.8	0.9989 0.9803	0.1290 0.1266	--	--	--	--	--	u_{fs} triples betw
steel +	38 (10° taper) 6	2.5[d]	17	7.80	5.4	O.L.	4.26	0.0060	2.0	0.9986	0.1280	--	--	--	--	--	u_{fs} rises 250% b

ror; O.L. = optical lever.
ved for Shots No. 8276-1, 8662, 8468.
ane-wave generator.

d. Assumed value, based on other shots.
e. Most uncertain values indicated by parentheses.
f. 4-inch explosive plane-wave generator.

g. Thickness at specimen.
h. See Table IV.